

Deep Signatures of Southern Tropical Indian Ocean Annual Rossby Waves*

GREGORY C. JOHNSON

NOAA/Pacific Marine Environmental Laboratory, Seattle, Washington

(Manuscript received 4 February 2011, in final form 12 April 2011)

ABSTRACT

The southern tropical Indian Ocean contains a striking forced annual Rossby wave studied previously using satellite altimeter sea surface height data, surface wind fields, expendable bathythermograph ocean temperature data, and models. Here, the deep reach of this wave and its velocity are analyzed using density–depth profiles and 1000-dbar horizontal drift data from Argo. Significant annual cycles in isopycnal vertical displacements and zonal velocity persist to the deepest pressures to which Argo data can be mapped reliably in the region, 1600–1900 dbar. Phase propagation of the annual cycle of the directly measured zonal velocities at 1000 dbar suggests a zonal wavelength of about 6000 km—about the length of the deep basin in which the wave is found—and a westward phase speed of $\sim 0.2 \text{ m s}^{-1}$. Apparent upward phase propagation in isopycnal vertical displacements suggests energy propagation downward into the abyss. This pattern is clearer when accounting for both the potential and kinetic energy of the wave. The largest zonal current associated with this wave has a middepth maximum that decays rapidly up through the pycnocline and less rapidly with increasing depth, suggesting a first-vertical-mode structure. The anomalous zonal volume transport of this annually reversing current is $\sim 27 \times 10^6 \text{ m}^3 \text{ s}^{-1}$ across 80°E in mid-November. The peak zonal velocity of 0.06 m s^{-1} implies a maximum zonal excursion of about 600 km associated with the wave over an annual cycle.

1. Introduction

A prominent annual signal within the southern tropical Indian Ocean (STIO) has been observed in sea surface height (SSH) anomalies from satellite altimeters (Périgaud and Delecluse 1992) as well as in thermocline depths expendable bathythermograph (XBT) data (Masumoto and Meyers 1998). A similar signal is also visible around $12^\circ\text{--}18^\circ\text{S}$ to a depth of 700 m in XBT data taken along $\sim 110^\circ\text{E}$, just west of Australia (Wijffels and Meyers 2004).

The annual signal in SSH anomalies in the STIO has a maximum along $\sim 12^\circ\text{S}$ that stretches across much of the Indian Ocean, strongest near 90°E (Périgaud and Delecluse 1992). Phase lines for the annual signal in SSH anomalies are oriented from west-northwest to east-southeast, as expected for Southern Hemisphere Rossby

waves, with a SSH maximum around May. XBT data show a similar picture, with maximum thermocline depth in November around 11°S , 90°E (Masumoto and Meyers 1998). The 180° phase difference for these two fields at maximum amplitude is expected, because a shallow thermocline corresponds to a low SSH. The small differences in patterns between these studies may be attributable to differences in spatial and temporal sampling for the XBTs and the altimeter.

This signal has been modeled as a near-resonant Rossby wave response to local seasonal winds (Masumoto and Meyers 1998), with a remotely forced contribution from the Pacific decaying westward from the west coast of Australia (Potemra 2001). A similar distinct annual Rossby wave has been observed and modeled farther to the west (Feng et al. 2010). This wave is discernable in the present analysis but only briefly noted here.

The analysis here uses Argo conductivity–temperature–depth (CTD) instrument profiles and horizontal drift data at 1000 dbar, the level at which most of the floats are configured to move with the ocean currents, to explore these annual signals in the STIO in both the density and the velocity fields. A large annual zonal velocity signal is apparent in the Argo float 1000-dbar horizontal drift data, as well as large annual signals in

* Pacific Marine Environmental Laboratory Contribution Number 3671.

Corresponding author address: Gregory C. Johnson, NOAA/Pacific Marine Environmental Laboratory, 7600 Sand Point Way N.E., Bldg. 3, Seattle, WA 98115.
E-mail: gregory.c.johnson@noaa.gov

isopycnal vertical displacements from the pycnocline all the way down to 1600–1900 dbar, the deepest reaches of the Argo floats. Section 2 describes the data used and their processing. Section 3 presents the analysis results, which are discussed in section 4.

2. Data, processing, and mapping

All Argo temperature T , salinity S , and pressure P data coded good (quality flag 1) were downloaded from an Argo Global Data Assembly Center in January 2011. Adjusted (delayed-mode quality controlled) data are used as available; otherwise, the real-time data are used. Potential temperature θ and potential density σ_θ are calculated and then S , θ , and P are linearly interpolated onto a set of σ_θ surfaces that span from the surface to 2000 dbar within the study region (20°S to the equator and 50°E to the west coasts of Indonesia and Australia). Argo float 1000-dbar horizontal drift data are also analyzed, in the form of the deep zonal U and meridional V velocities as estimated by Lebedev et al. (2007), updated through January 2011. Finally, a monthly climatology of wind stress curl derived from September 1999–October 2009 satellite scatterometer winds (Risien and Chelton 2008) is used here.

For the analysis, we map the data to a regular latitude–longitude grid using a weighted quadratic (a Loess filter) with added annual and semiannual harmonics. We employ a 200-km meridional scale and a 1000-km zonal scale for the filter. We eliminate extreme outliers by calculating the interquartile range (IQR) for salinity and pressure within range of each grid point and discarding any values 3 times the IQR less than the first quartile or 3 times the IQR greater than the third quartile. For U and V , we discard mapped values at grid points with the sum of the weights < 150 or a weighted centroid of data $> 1/3$ of the distance from grid point in terms of smoothing scales. We discard similarly for θ , S , and P , but with weight sums < 200 . We also discard values for any grid points mapped to below the ocean floor or above the ocean surface and any grid points with a density lighter than the local (similarly mapped) annual maximum in mixed layer density. We retain all values from the monthly wind stress curl climatology to use for its mapping.

The annual cycle of referenced geostrophic zonal velocity is computed by first transforming the means and annual harmonics of isopycnal pressures back to density on pressure coordinates at monthly resolution. For each month, horizontal density gradients are computed by centered differences then these gradients are integrated vertically, applying the thermal wind relation to get zonal velocities. Finally these zonal velocities are referenced to the 1000-dbar level of known motion from

the Argo float horizontal drift data, using their means and annual harmonics for the reference.

For some presentations of isopycnal vertical displacements, zonal velocities, and isopycnal pressures, Wentzel–Kramers–Brillouin–Jeffreys (WKBJ) stretching and scaling is applied to account for the effects of varying stratification with depth on planetary wave propagation and signatures (e.g., Eriksen 1981). To compute a mean buoyancy frequency N profile as a function of density for this scaling, first the mean pressure (ranging from 54 to 1960 dbar) of each isopycnal within the study region is computed from the gridded maps. Values of N are then estimated at midpoints between these isopycnals. The pressure average of N , $N_o = 3.7 \times 10^{-3} \text{ s}^{-1}$, is located near 400 dbar in the mean profile. Then, N and N_o are used to obtain scaled vertical isopycnal displacement values ς , scaled U values, and stretched pressure for the vertical coordinate of the plots of that quantity. The relation for scaled total energy, $0.5 \times (N_o^2 \times \varsigma^2 + U^2)$, is also used in conjunction with the annual harmonics for ς and U .

3. Results

The quantity ς has a strong annual cycle in the pycnocline, including a zonally elongated patch with a maximum amplitude exceeding 50 scaled dbar on $\sigma_\theta = 25.0 \text{ kg m}^{-3}$ (Fig. 1a) that extends from 11°S, 95°E to about 8°S, 75°E. Lines of constant phase of ς are oriented west-northwest to east-southeast, so phase propagation is south-southwest, with the meridional maximum consistently occurring around mid-November along the maximum amplitude of the patch. On this isopycnal, the annual cycle accounts for up to 50% of the total variance (not shown) of ς around the patch maximum and fades to $< 10\%$ outside the thick black lines.

The phase and amplitude patterns of the annual cycle of the wind stress curl (Fig. 1b) are consistent with it driving much of the annual cycle of pycnocline displacement observed from the isopycnal vertical displacement data. A zonally elongated maximum in amplitude along 10°S extends from 90° to 110°E around September. Following Rossby wave characteristics westward through this pattern in wind stress curl would result in an increasingly strong annual isopycnal vertical displacement, peaking around 10°S, 90°E a few months after September, corresponding to what is observed (Fig. 1a). This result is not surprising in light of previous studies showing the importance of a near-resonant forced Rossby wave response to seasonal wind variations in the pycnocline in the region (Masumoto and Meyers 1998; Potemra 2001), but here Argo data allow study of these patterns well below the pycnocline,

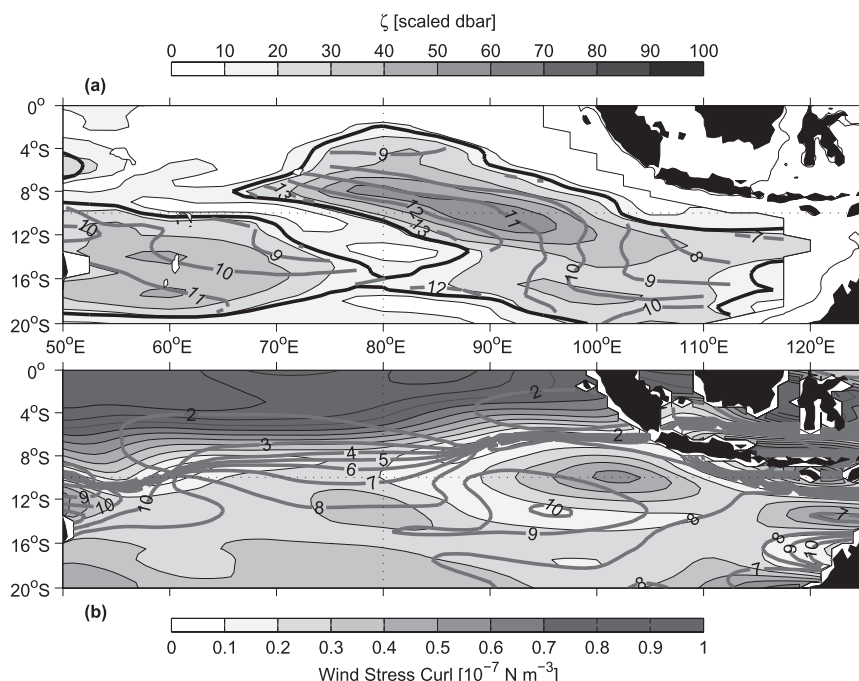


FIG. 1. (a) Phase (thick gray contours, labeled at midmonth so that 11 = 15 Nov, etc.) and amplitude (top grayscale bar) of the annual cycle of scaled isopycnal displacement ζ on $\sigma_\theta = 25.0 \text{ kg m}^{-3}$. Regions where the annual signal explains over 10% of the variance are outlined (thick black contours), and phase is shown only inside these regions. (b) Phase (thick gray contours, labeled as above) and amplitude (bottom grayscale bar) of the annual cycle of wind stress curl. Bathymetry is masked with white, and land is masked with black. Thin dotted lines indicate positions of sections along 80°E (Figs. 2, 5) and 10°S (Figs. 3, 6).

approaching 2000 dbar. The broad maximum in ζ amplitude around 16°S, 60°E (Fig. 1a) could similarly be driven by the broad maximum in wind stress curl located a few thousand kilometers to the east of its center (Fig. 1b; Feng et al. 2010).

The November maximum in the annual cycle of ζ persists from the surface to at least the 1900-dbar reach of Argo along 80°E (Fig. 2), with clear southward phase propagation at all depths. Along this longitude, the region with strongest signal is confined to about 900 km in the north–south direction (much larger than the 200-km meridional mapping scale). The latitude of the ζ maximum appears to shift southward (along with its phase) with increasing depth from about 8° to about 12°S around $\sigma_\theta \sim 27.0 \text{ kg m}^{-3}$ ($P \sim 600$ dbar). The amplitude of the annual cycle of ζ exhibits a minimum around the density (and pressure) of this shift. The annual cycle accounts for over 40% of the variance of ζ at the peak of the shallow maximum and over 30% around the peak of the deeper maximum.

Many similar features are evident in the annual cycle of ζ along 10°S (Fig. 3), including the November maximum from the surface to 2000 dbar. There is clear westward phase propagation at all depths. Along this

latitude, the region with strongest signal is confined to about 4000 km in the east–west direction (again, much larger than the 1000-km zonal mapping scale). The longitude of the ζ maximum appears to shift westward with increasing depth (again, retaining its phase) from about 90° to about 75°E. Again, much of the shift occurs around $\sigma_\theta \sim 27.0 \text{ kg m}^{-3}$ ($P \sim 600$ dbar), where the amplitude of the annual cycle of ζ is a minimum. The annual cycle of ζ accounts for over 60% of the variance at the peak of the shallow maximum and over 40% around the peak of the deeper maximum. The distinct western Rossby wave (mentioned above but not analyzed here) is apparent within the pycnocline from 50° to 70°E.

Along both 80°E (Fig. 2) and 10°S (Fig. 3), there is some evidence in ζ for upward phase propagation, but it appears far from uniform vertically within the high signal regions, even in stretched pressure coordinates. Phase apparently shifts near $\sigma_\theta \sim 27.0 \text{ kg m}^{-3}$ ($P \sim 600$ dbar), where the amplitude of the annual cycle of ζ is also a minimum. However, the potential energy in ζ is not the only component of Rossby wave energy. As shown below, consideration of the contributions of kinetic energy—using geostrophic zonal velocity relative to a level of known motion from the floats—reduces the

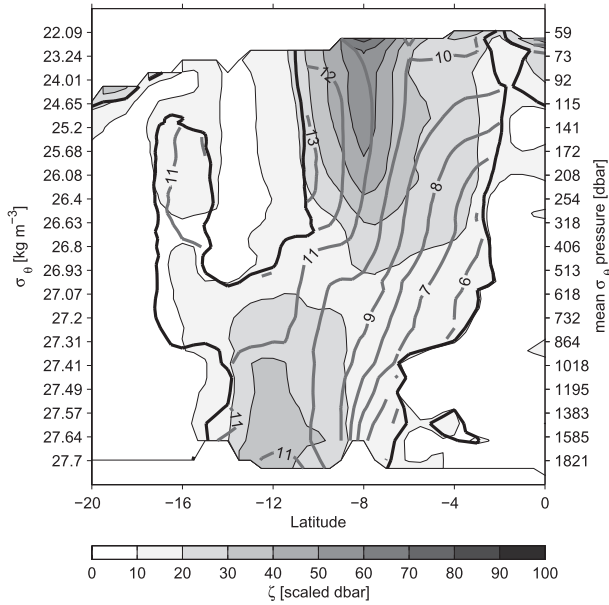


FIG. 2. Phase (thick gray contours) and amplitude (grayscale bar) of the annual cycle of scaled isopycnal vertical displacement ζ along 80°E (see vertical thin dotted lines in Figs. 1, 4 for location). Vertical axis is mean stretched pressure of isopycnals, where left labels indicate isopycnals and right labels indicate actual (unscaled) mean pressure of isopycnals. Other details as in Fig. 1.

middepth minimum in amplitude, as well as the abruptness of the phase shift.

The annual cycle of ζ on $\sigma_\theta = 27.4 \text{ kg m}^{-3}$ (Fig. 4a)—the isopycnal with a mean pressure closest to 1000 dbar in the study region—has a zonally elongated patch with a maximum amplitude exceeding 30 stretched dbar along 12°S from 70° to 85°E in November. This pattern is shifted to the west and slightly to the south of that in the pycnocline (Fig. 1a), which is consistent with the sections (Figs. 2, 3). Lines of constant phase for ζ are again oriented west-northwest to east-southeast, so phase propagation is south-southwest. The maximum amplitude of annual cycle of ζ on this isopycnal is also smaller than in the pycnocline, which is consistent with the sections. The annual cycle accounts for over 30% of the variance of ζ at 1000 dbar near its peak. This percentage is not large, likely because the 1000-dbar level is at the bottom edge of the middepth amplitude minimum in the annual cycle of ζ (Figs. 2, 3).

The annual cycle in U directly estimated from the Argo 1000-dbar horizontal drift data (Fig. 4b) also shows a zonally elongated patch with maximum amplitude exceeding 0.04 m s^{-1} that extends from 8°S , 67°E to 10°S , 87°E . This feature lies about 300 km north of the maximum amplitude of the annual cycle in ζ . Phase propagation for the annual cycle in U at 1000 dbar is again south-southwest. Fitting a plane wave to the phase of the annual

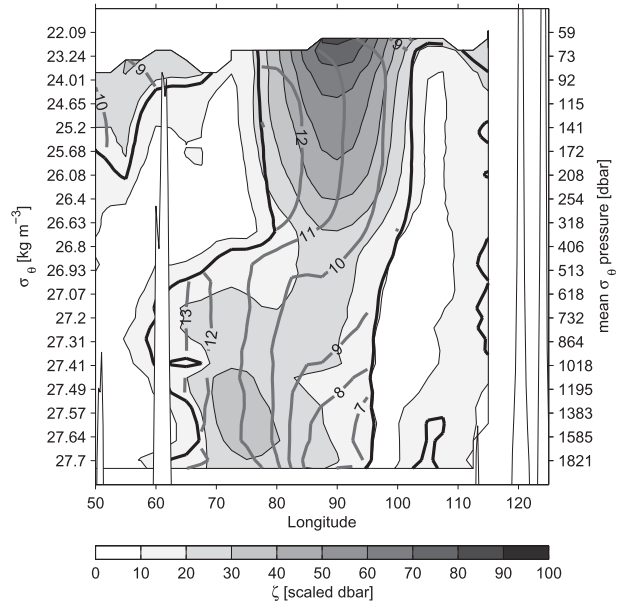


FIG. 3. Phase and amplitude of the annual cycle of scaled isopycnal vertical displacement ζ along 10°S (see horizontal thin dotted lines in Figs. 1, 4 for location). Bathymetry is masked with white. Other details as in Fig. 2.

cycle of U at 1000 dbar within its main patch yields a relatively short meridional wavelength ($\sim 1000 \text{ km}$) and longer zonal wavelength ($\sim 6000 \text{ km}$). The phase of maximum amplitude in U is around mid-May, meaning that maximum eastward velocities at 1000 dbar are associated with the maximum shoaling of isopycnals to the south at that time of the year. The thermal wind relation also suggests increasing relative eastward flow at shallower depths around this pressure at that time. This result is consistent with a maximum in the zonal velocity signature of the wave for pressures shallower than 1000 dbar, as illustrated below. The annual cycle accounts for over 50% of the variance of U at 1000 dbar around its peak.

The annual cycle in V at 1000 dbar (not shown) is also zonally elongated, with about one-fifth the amplitude of that for U as expected from the ratio of zonal to meridional wavelengths estimated above. The pattern for V is spatially coincident with that for ζ on $\sigma_\theta = 27.4 \text{ kg m}^{-3}$. However, the variance of V explained by the annual cycle barely rises above 10% anywhere. Given its small amplitude and low signal-to-noise ratio, we do not consider V further.

The estimates of the annual cycle in zonal velocity at 1000 dbar (a level of known motion estimated from the Argo 1000-dbar horizontal drift data) are combined with the annual cycle of isopycnal depths (which give geostrophic shear by the thermal wind) as outlined in section 2, to gain a picture of the anomalous zonal velocities associated with this annual Rossby wave. The zonal

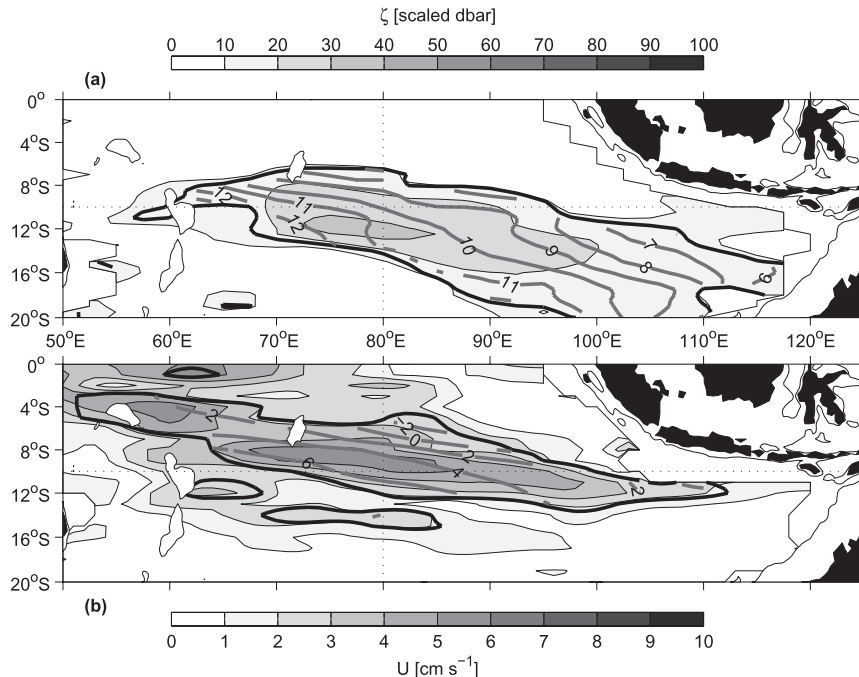


FIG. 4. (a) Phase and amplitude of the annual cycle of scaled isopycnal vertical displacement ς on $\sigma_\theta = 27.4 \text{ kg m}^{-3}$ (~ 1000 dbar). (b) Phase and amplitude of the annual cycle of unscaled zonal velocity U at 1000 dbar. Other details as in Fig. 1.

velocity anomaly in mid-November along 80°E (Fig. 5) shows a westward jet with peak velocity of 0.06 m s^{-1} near 9°S , 600 dbar. This westward jet persists into the pycnocline and even to the bottom of the sampling depth of Argo, suggesting a first-vertical-mode structure for the Rossby wave. The depth of the maximum amplitude in the annual cycle of U lies near the minimum in amplitude for ς , so kinetic energy is an important contributor to the total energetics of the wave at this depth. The jet is flanked to the north and south by jets with peak velocities exceeding 0.03 m s^{-1} (around 6°S , 1000 dbar) and 0.02 m s^{-1} (around 14°S , 600 dbar), respectively. November is chosen to illustrate the westward jet near its maximum amplitude, but the eastward jets that flank it peak at different times of the year.

Integrating this directly referenced westward zonal velocity anomaly in mid-November (Fig. 5) for $\sigma_\theta > 26.2 \text{ kg m}^{-3}$ to the bottom of the map (around 1600–1800 dbar, depending on latitude) from 13° to 5°S yields an anomalous volume transport of $-27 \times 10^6 \text{ m}^3 \text{ s}^{-1}$ through 80°E . A similar calculation for the northern jet in mid-November suggests $9 \times 10^6 \text{ m}^3 \text{ s}^{-1}$ of eastward transport and for the southern jet suggests $10 \times 10^6 \text{ m}^3 \text{ s}^{-1}$.

As foreshadowed above, the amplitude and phase of the combined of the annual harmonics of the scaled isopycnal displacement and the scaled zonal velocity divided by the reference buoyancy frequency,

$\varsigma - U \times N_o^{-1}$, accounts for both the potential and kinetic energy contributions to the annual STIO Rossby wave, yielding a clearer picture of its amplitude and phase. For instance, along 10°S (Fig. 6) the amplitude of this combination is still largest near the surface, but the signal is everywhere stronger for the combination and its mid-depth minimum is not as pronounced as that of ς alone (Fig. 3). (Note that the centered differences used in estimating geostrophic velocity do limit the area over which the combination can be estimated.) The phase of the combination also shifts much more smoothly westward with increasing depth throughout the water column than does that of ς alone. This pattern is expected for a first vertical mode in geostrophic balance, with much of the kinetic energy at middepth and much of the potential energy above and below. A similar improvement in the continuity of both amplitude and phase occurs when considering the combination of the kinetic and potential components of the wave along 80°E (not shown) and presumably elsewhere.

4. Discussion

The wind stress, Argo horizontal drift data, and Argo density profile data analyzed here all combine to yield a dynamically consistent picture of an annual Rossby wave forced by the seasonal cycle of winds in the

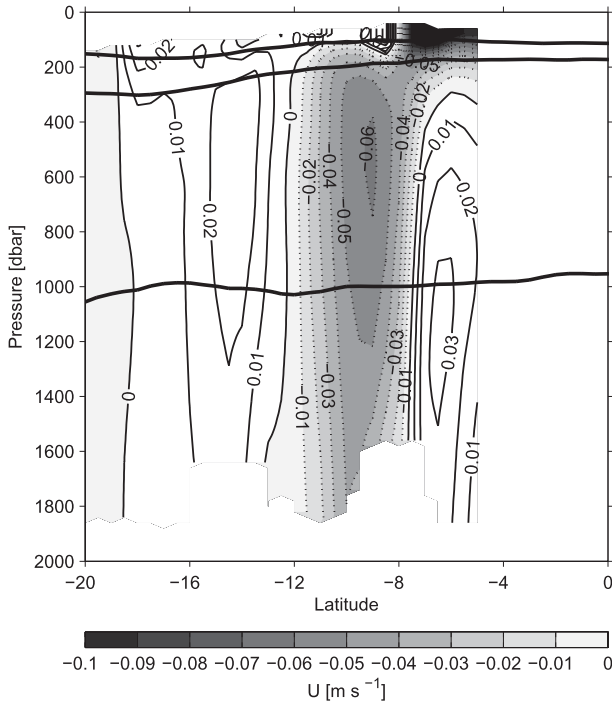


FIG. 5. Unscaled zonal velocity anomaly U for mid-November along 80°E from annual cycles fit to Argo density profile and 1000-dbar horizontal drift data (see vertical thin dotted lines in Figs. 1, 4 for location). Negative values are shaded increasingly gray (grayscale bar) and contoured with thin dashed lines. Positive values are unshaded and contoured with thin solid lines. Contours of the mean positions of $\sigma_\theta = 27.4, 26.2,$ and 25.0 kg m^{-3} are also shown (thick black lines). Geostrophic velocities are not shown north of 5°S , because they become increasingly unrealistic approaching the equator.

eastern south tropical Indian Ocean. As some of its energy propagates westward and down into the abyss, this wave has a reach deeper even than that of Argo floats. Although the wave has been studied before and its deep reach is to be expected dynamically, we are not aware that its deep signatures in density and velocity have been described previously.

Along 80°E , the anomalous westward velocities associated with this wave peak at about 0.06 m s^{-1} at middepth (around 500 dbar) and 9°S in mid-November and still exceed 0.04 m s^{-1} at 1800 dbar, the maximum pressure to which the density field can be reliably mapped with Argo data. Thus, the $-27 \times 10^6 \text{ m}^3 \text{ s}^{-1}$ anomalous westward transport found below the pycnocline across this longitude in mid-November is an underestimate of the full transport anomaly, because westward velocities likely persist to well below the maximum sampling pressure of Argo floats. Hence, an assumption of a deep level of no motion (e.g., at 700 or even 2000 dbar) would yield quite erroneous results regarding velocities associated with this wave. This

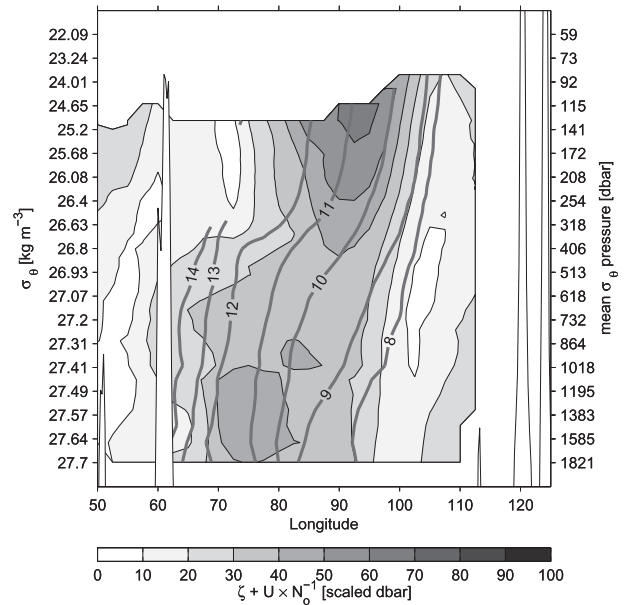


FIG. 6. Phase (thick gray contours) and amplitude (grayscale bar) of the combined annual cycles of scaled isopycnal vertical displacement and scaled zonal velocity divided by the reference buoyancy frequency, $s - U \times N_o^{-1}$, along 10°S (see horizontal thin dotted lines in Figs. 1, 4 for location). Other details as in Fig. 2, but phase is contoured only for amplitudes > 5 scaled dbar and the 10% variance outline is omitted.

seasonal variation in transport associated with the annual Rossby wave is large, on the order of estimates of the overlying westward transport of the South Equatorial Current in the upper 400 m (Gordon et al. 1997). Furthermore, the zonal excursion of a water parcel at the velocity maximum of this Rossby wave (absent the mean flow or other influences) could be as much as 600 km over half a year, with return over the other half.

The middepth maximum in the annual cycle of zonal velocities (Fig. 5) at 9°S , 500 dbar along 80°E corresponds to the middepth minimum in the annual cycle of s (Fig. 2). The geostrophic relation links these patterns: isopycnals anomalously deepen to the south of the core below it in November, reducing westward velocities with increasing depth below the core. They also deepen to the north of the core above it, reducing westward velocities toward the surface above the core. The middepth maximum in zonal velocity, a signature of the first-vertical-mode structure of the Rossby wave, would be difficult to discern using XBT data, which only reach to about 700 dbar, even if the reference velocities were perfectly known.

The isopycnal vertical displacements and zonal velocities also complement each other in terms of energy. Where the potential energy of the wave as seen in the annual cycle of s is a minimum (Fig. 2), the kinetic energy is a maximum, as seen in the zonal velocity of the

annual cycle of the wave (Fig. 5). With WKBJ scaling, the potential and kinetic energy terms are of comparable magnitude, and they combine to make a relatively smooth and coherent picture of downward and westward (Fig. 6) energy propagation.

At the eastern end of this analysis, the annual signal in ζ and U is discernible to almost 120°E as early as June–July (Figs. 1a, 4), too early in the year and too far east to be forced by the interior wind stress curl patch, which peaks in September and only reaches as far east as 110°E (Fig. 1b). Previous studies attribute this eastern annual Rossby wave signature to energy from annual remote forcing in the Pacific radiating westward from the west coast of Australia (Potemra 2001; Wijffels and Meyers 2004).

At the western end of this analysis, the Rossby wave signatures do not appear to reach west of about 65°E (Figs. 3, 4), the longitude of the Mascarene Plateau. Because the wind forcing that this Rossby wave carries westward and into the abyss is concentrated east of 90°E, the plateau apparently blocks the signal, which is too deep to pass over it when it reaches that longitude.

The zonal wavelength of the annual Rossby wave as estimated from a plane fit to the annual cycle of directly measured zonal velocity at 1000 dbar is ~ 6000 km, implying a zonal phase speed of ~ 0.2 m s⁻¹ westward. The estimated zonal wavelength is just about the length of the deep basin along 10°S from the Mascarene Plateau to the continental shelf of northwest Australia. Thus, the wave appears to span the basin both vertically (with its first-vertical-mode structure) and zonally.

Acknowledgments. Float data used here were collected and made freely available by Argo (<http://www.argo.net/>), a program of the Global Ocean Observing System, and contributing national programs. This study used the data of YoMaHa'07 (Lebedev et al. 2007),

velocities derived from Argo float trajectories and provided by APDRC/IPRC. Discussions with LuAnne Thompson, John Lyman, and Dennis Moore were helpful. Comments from Kevin Speer and one anonymous reviewer also improved the manuscript. The NOAA Office of Oceanic and Atmospheric Research supported this research.

REFERENCES

- Eriksen, C. C., 1981: Deep currents and their interpretation as equatorial waves in the western Pacific Ocean. *J. Phys. Oceanogr.*, **11**, 48–70.
- Feng, J., X. Bai, Y. Chen, and D. Hu, 2010: Effect of low-frequency Rossby wave on thermal structure of the upper southwestern tropical Indian Ocean. *Chin. J. Oceanol. Limnol.*, **28**, 344–353.
- Gordon, A. L., S. Ma, D. B. Olson, P. Hacker, A. Field, L. D. Talley, D. Wilson, and M. Baringer, 1997: Advection and diffusion of Indonesian Throughflow Water within the Indian Ocean South Equatorial Current. *Geophys. Res. Lett.*, **24**, 2573–2576.
- Lebedev, K., H. Yoshinari, N. A. Maximenko, and P. W. Hacker, 2007: YoMaHa'07: Velocity data assessed from trajectories of Argo floats at parking level and at the sea surface. IPRC Tech. Note 4(2), 16 pp.
- Masumoto, Y., and G. Meyers, 1998: Forced Rossby waves in the southern tropical Indian Ocean. *J. Geophys. Res.*, **103**, 27 589–27 602.
- Périgaud, C., and P. Delecluse, 1992: Annual sea level variations in the southern tropical Indian Ocean from Geosat and shallow-water simulations. *J. Geophys. Res.*, **97**, 20 169–20 178.
- Potemra, J., 2001: Contribution of equatorial Pacific winds to southern tropical Indian Ocean Rossby waves. *J. Geophys. Res.*, **106**, 2407–2422.
- Risien, C. M., and D. B. Chelton, 2008: A global climatology of surface wind and wind stress fields from eight years of QuikSCAT scatterometer data. *J. Phys. Oceanogr.*, **38**, 2379–2413.
- Wijffels, S., and G. Meyers, 2004: An intersection of oceanic waveguides: Variability in the Indonesian Throughflow region. *J. Phys. Oceanogr.*, **34**, 1232–1253.